Mice Genetically Deficient in Vasopressin V1a and V1b Receptors Are Resistant to Jet Lag

Yoshiaki Yamaguchi,[1]* Toru Suzuki,[1]* Yasutaka Mizoro,[1] Hiroshi Kori,[2,3] Kazuki Okada,[1] Yulin Chen,[1] Jean-Michel Fustin,[1] Fumiyoshi Yamazaki,[1] Naoki Mizuguchi,[1] Jing Zhang,[4] Xin Dong,[4] Gozoh Tsujimoto,[5] Yasushi Okuno,[6] Masao Doi,[1] Hitoshi Okamura[1,4]†

Jet-lag symptoms arise from temporal misalignment between the internal circadian clock and external solar time. We found that circadian rhythms of behavior (locomotor activity), clock gene expression, and body temperature immediately reentrained to phase-shifted light-dark cycles in mice lacking vasopressin receptors V1a and V1b ($V1a^{-/-}V1b^{-/-}$). Nevertheless, the behavior of $V1a^{-/-}V1b^{-/-}$ mice was still coupled to the internal clock, which oscillated normally under standard conditions. Experiments with suprachiasmatic nucleus (SCN) slices in culture suggested that interneuronal communication mediated by V1a and V1b confers on the SCN an intrinsic resistance to external perturbation. Pharmacological blockade of V1a and V1b in the SCN of wild-type mice resulted in accelerated recovery from jet lag, which highlights the potential of vasopressin signaling as a therapeutic target for management of circadian rhythm misalignment, such as jet lag and shift work.

The endogenous circadian clock drives oscillations in physiology and behavior with a period of about 24 hours. We are not usually aware of this system because it is completely synchronized with environmental light-dark cycles, but travelling rapidly across multiple time zones suddenly makes us aware of the desynchrony, causing sleep disturbances and gastrointestinal distress (*1*, *2*). Repeated jet-lag exposure and rotating shift work increase the risk of lifestyle-related diseases, such as cardiovascular complaints and metabolic insufficiency (*3*, *4*). Although jet lag is recognized as a chronobiological problem (*5*–*7*), its specific molecular and cellular mechanisms are poorly understood.

In mammals, internal time is orchestrated by the master clock in the hypothalamic suprachiasmatic nucleus (SCN), whose coherent output signal synchronizes cell clocks throughout the body (*8*–*13*). Hence, a misalignment of SCN clock signals and environmental time cues (e.g., light and temperature) would occur during jet lag. To identify candidate signaling molecules that might contribute to jet lag, we designed a screening strategy (*14*) in which we (i) used histochemistry to identify genes whose expression is enriched in the mouse SCN, (ii) generated mutant mice lacking candidate genes of interest, and (iii) measured the locomotor activity of the mutant mice under experimental jet-lag conditions. Genes encoding brain peptides and their receptors were the initial candidates of interest, because many of them are expressed in the SCN (*15*). We identified arginine vasopressin (AVP) and its receptors (V1a and V1b receptors) as strong candidates. The circadian expression pattern of these proteins has been studied (*16*–*18*), but their role in the circadian clock is unclear, with the exception of the V1a receptor. Genetic deletion of this receptor causes period elongation in mice (*19*).

Locomotor Activities During Jet Lag

We generated V1a and V1b receptor double-knockout mice ($V1a^{-/-}V1b^{-/-}$ mice) (*20*–*22*) and examined their behavioral rhythms under experimental jet-lag conditions. The mice were housed in a light (~200 lux)–controlled isolator with food and drink ad libitum, and their spontaneous locomotor activity was recorded by infrared sensor (Fig. 1, A to C) or voluntary wheel running (fig. S1). When they were maintained in a 12-hour light/12-hour dark (LD) cycle, both wild-type (WT) and $V1a^{-/-}V1b^{-/-}$ mice exhibited high locomotor activity during the dark phase. After 2 weeks of recording behaviors, LD cycles were advanced by 8 hours. In WT mice, this advance evoked a gradual shift of locomotor activity rhythms, which took 8 to 10 days for complete reentrainment to the new LD schedule (Fig. 1, A and B). This slow resetting of locomotor activity rhythm—which is characterized by an activity onset that is not synchronous with "lights off" as normally observed, but is delayed into the night—was expected, as it is the typical sign that mice are experiencing jet lag. Every subsequent day after the LD cycle advance, the WT mice will start their activity slightly earlier, to finally align, after 8 to 10 days, to the beginning of the night. In contrast, $V1a^{-/-}V1b^{-/-}$ mice showed almost immediate reentrainment with only 2 to 4 days of transition (Fig. 1A).

For quantitative comparison between genotypes, we calculated the 50% phase-shift value (PS_{50}) (*5*) and found that $V1a^{-/-}V1b^{-/-}$ mice reentrained more rapidly than WT mice (Fig. 1B, inset) ($P < 0.001$, unpaired t test). We then delayed LD cycles by 8 hours (Fig. 1, A and C) and found that, although WT mice required 5 to 6 days for reentrainment, $V1a^{-/-}V1b^{-/-}$ mice required only 1 day (Fig. 1, A and C), and PS_{50} was also much smaller in $V1a^{-/-}V1b^{-/-}$ mice (Fig. 1C, inset) ($P < 0.001$, unpaired t test). We next examined which AVP receptor, V1a or V1b, dictates the rate of reentrainment after phase shift and found that single knockout ($V1a^{-/-}V1b^{+/+}$ mice and $V1a^{+/+}V1b^{-/-}$) mice showed intermediate rates of reentrainment (figs. S2 and S3), which indicated that both receptors contribute to the accelerated reentrainment after jet lag.

Light has a dominant influence on the behavior of mice because they are nocturnal animals; it inhibits their locomotor activity or foraging behavior. To exclude the possibility that the locomotor activity of $V1a^{-/-}V1b^{-/-}$ mice is merely caused by the ambient LD cycle, we released mice in constant darkness (DD) after a transient advance in LD cycles. After 4, 3, 2, and only 1 day advance in the LD cycle, larger phase advances in the free-running behavior of $V1a^{-/-}V1b^{-/-}$ mice were observed compared with WT mice (Fig. 1, D to F, and fig. S4). $V1a^{-/-}V1b^{-/-}$ mice also showed larger phase delays in behavior after only 1 day's delay in LD cycles (fig. S5). These findings strongly suggest that the immediate adaptation to a new LD cycle in $V1a^{-/-}V1b^{-/-}$ mice is not a masking effect of the environmental LD cycle but a rapid phase shift of the endogenous clock. Of note, period length in DD conditions, phase angle from LD to DD, phase response curve obtained with a short light exposure, and expression of canonical clock genes (*Per1*, *Per2*, *Bmal1*, and *Dbp*) in $V1a^{-/-}V1b^{-/-}$ SCN were virtually identical to those in WT mice (Fig. 1, G to J, and figs. S6 and S7). These behavioral and molecular data exclude the possibility that rapid reentrainment in $V1a^{-/-}V1b^{-/-}$ mice is simply caused by a disabled clock. When behavioral experiments were performed under conditions of intermediate light intensity (~50 lux), we also found that $V1a^{-/-}V1b^{-/-}$ mice reentrained faster after a phase advance or phase delay (figs. S8 and S9) and showed larger phase advances after a 1- to 4-day advance in LD cycles (fig. S10). Moreover, there were no significant differences between genotypes in the phase delay in locomotor activities, the level of *Per1* induction, or the number of *Per1*-positive cells induced by a light pulse at CT14 (CT represents circadian time; CT0 is subjective dawn and CT12 is subjective dusk) (fig. S11), which suggested that the light response of $V1a^{-/-}V1b^{-/-}$ SCN clock is similar to that of WT.

[1]Department of Systems Biology, Graduate School of Pharmaceutical Sciences, Kyoto University, Sakyo-ku, Kyoto 606-8501, Japan. [2]Department of Information Sciences, Ochanomizu University, Tokyo 112-8620, Japan. [3]CREST, Japan Science and Technology Agency, Kawaguchi, Saitama 332-0012, Japan. [4]Division of Molecular Brain Science, Department of Brain Science, Kobe University Graduate School of Medicine, Chuo-ku, Kobe 650-0017, Japan. [5]Department of Genomic Drug Discovery Science, Graduate School of Pharmaceutical Sciences, Kyoto University, Kyoto 606-8501, Japan. [6]Department of Systems Biosciences for Drug Discovery, Graduate School of Pharmaceutical Sciences, Kyoto University, Kyoto 606-8501, Japan.

*These authors contributed equally to this work.
†Corresponding author. E-mail: okamurah@pharm.kyoto-u.ac.jp

Oscillations of Clock Genes During Jet Lag

To characterize molecular changes in the SCN during jet lag, we examined clock gene expression in laser-microdissected SCN samples collected from mice killed every 4 hours (fig. S12). Before a phase advance in LD cycles, all transcripts examined in both genotypes showed a similar expression pattern: *Per1*, *Per2*, and *Dbp* showed comparable peak values around the middle of the day, ZT6 to ZT10 (ZT represents Zeitgeber time used in LD cycle; ZT0 is lights-on and ZT12 is lights-off), whereas *Bmal1* was highest around ZT14 (Fig. 2). In contrast, after a phase advance in LD cycles, there were striking differences between genotypes in clock gene

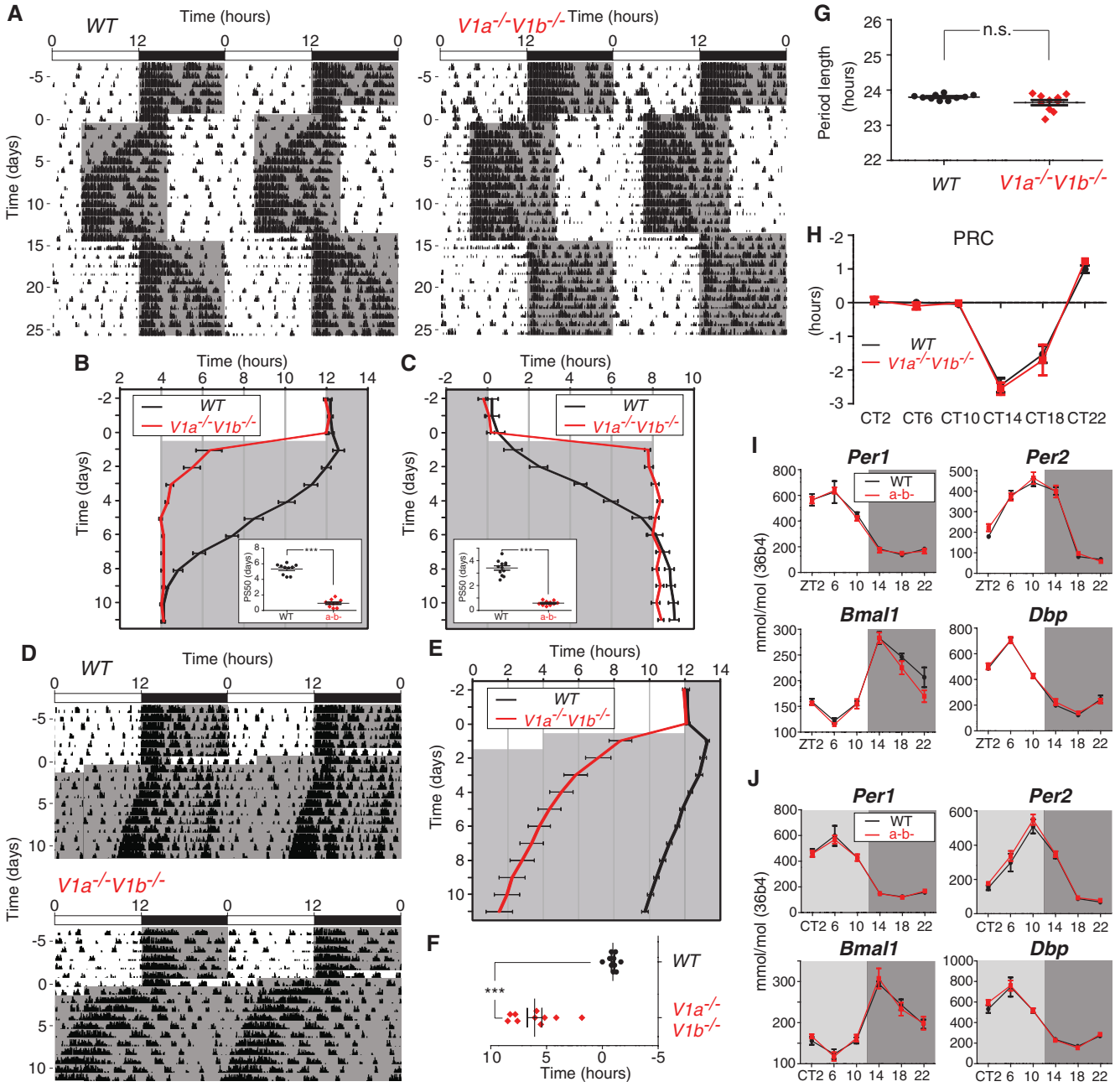

Fig. 1. *V1a*$^{-/-}$*V1b*$^{-/-}$ mice subjected to an experimental jet-lag paradigm show immediate reentrainment to a new light-dark cycle. (**A**) Representative double-plotted actogram of WT (left) and *V1a*$^{-/-}$*V1b*$^{-/-}$ (right) mice subjected to an 8-hour phase advance and delay in LD cycles. (**B**) Activity onset in the 8-hour phase advance [means ± SEM; $n = 10$ (both genotypes)]. (**C**) Activity offset in 8-hour phase delay [means ± SEM; $n = 12$ (WT) and 10 (*V1a*$^{-/-}$*V1b*$^{-/-}$)]. Insets (B and C) indicate PS_{50} values in phase advance and in phase delay (means ± SEM; ***$P < 0.001$, unpaired *t* test). (**D** to **F**) Representative double-plotted actograms (D) of WT (top) and *V1a*$^{-/-}$*V1b*$^{-/-}$ mice (bottom) subjected to an 8-hour phase advance on day 1 and released to DD, activity onset (E) and magnitude of the phase advance (F) [means ± SEM; $n = 10$ (both genotypes); ***$P < 0.001$, unpaired *t* test]. (**G**) Period length of WT and *V1a*$^{-/-}$*V1b*$^{-/-}$ mice, based on a 14-day interval taken after 3 days of a DD regime. Plotted are the period lengths of individual animals [means ± SEM; $n = 10$ (both genotypes); $P = 0.9524$, unpaired *t* test]. (**H**) Quantification of the magnitude of phase shifts by a brief light exposure (30 min of ~200 lux fluorescent light at CT2, 6, 10, 14, 18, and 22; $n = 8$ for both genotypes). By convention, delays are negative and advances are positive. Note that WT and *V1a*$^{-/-}$*V1b*$^{-/-}$ mice have virtually the same phase-shift magnitude at all time points. (**I** and **J**) Clock gene expression in the SCN in LD (I) and in DD (J) conditions. SCN was dissected out by laser microdissection (see fig. S8), and each transcript was measured by quantitative reverse transcription polymerase chain reaction (qRT-PCR) [means ± SEM; $n = 5$ (both genotypes in both LD and DD)]. For this and subsequent figures, white and gray background indicates lights on and off, respectively. Black and red colors indicate WT and *V1a*$^{-/-}$*V1b*$^{-/-}$, respectively. Top bars indicate initial LD cycle.

expression. In WT mice, *Per1* and *Per2* expression lost rhythmicity on days 1 to 2, oscillated with very low amplitude on days 3 to 7, and recovered to the original circadian expression pattern on day 8. *Bmal1* and *Dbp* expression also required 8 to 9 days for complete recovery to the original circadian expression pattern, with severely perturbed rhythmicity on days 1 to 5 (Fig. 2). In $V1a^{-/-}V1b^{-/-}$ mice, although the expression of some genes was partially perturbed on days 1 to 2, the peak time and amplitude in oscillations of all four clock genes recovered on day 3 (Fig. 2). Consistent with these results, cellular level analysis by digoxigenin in situ hybridization revealed that the robust oscillation in *Per1* and *Dbp* in WT SCN was severely perturbed on day 3 after a phase advance in LD cycles but not in $V1a^{-/-}V1b^{-/-}$ SCN (fig. S13).

We next examined the phase-transition kinetics of clock gene rhythms in peripheral organs and monitored temperature rhythms. In contrast to what we observed with the SCN, clock gene rhythm amplitudes in the liver were maintained during reentrainment. However, the peak time was severely affected after a phase advance in LD cycles: phase recovery required 9 to 10 days in WT mice but only 5 days in $V1a^{-/-}V1b^{-/-}$ mice (Fig. 3, A and B). Similar reentrainment kinetics was also observed in the kidney (fig. S14). Body temperature rhythms peaking at ZT16 reentrained within 5 days in $V1a^{-/-}V1b^{-/-}$ mice, but needed 10 days in WT mice after a phase advance in LD cycles (Fig. 3, C and D). These results demonstrate the rapid reentrainment of clock gene and body temperature rhythms in $V1a^{-/-}V1b^{-/-}$ mice (see supplementary text for comparison with previous jet-lag studies in WT mice). In addition, reestablishment of the central SCN clock occurred 1 to 2 days earlier than that of the peripheral clock or body temperature rhythms in both genotypes, which suggests that the SCN clock determines the recovery period of the whole body.

Vasopressin Signaling and Interneuronal Communication in the SCN

It is well established that AVP neurons constitute the main population of the SCN and that AVP synthesis and release from the SCN to the cerebrospinal fluid exhibit a robust circadian rhythm (*16*, *23*). AVP neurons mutually connect via synaptic contacts and form a local circuit within the SCN (*24*). *V1a* and *V1b* are expressed in SCN neurons (*25*), and our double in situ hybridization results revealed that most AVP neurons also expressed *V1a* in the dorsomedial SCN (fig. S15, A to D), which indicated abundant interactions between AVP neurons. Moreover, transcripts of *AVP* and *V1a* showed robust antiphasic rhythms (fig. S15, E and F), which suggested dynamic circadian regulation of ligand-receptor interactions (*12*).

We hypothesized that the disruption of clock gene rhythms observed in WT SCN, but not in $V1a^{-/-}V1b^{-/-}$ SCN, during jet lag might be due to

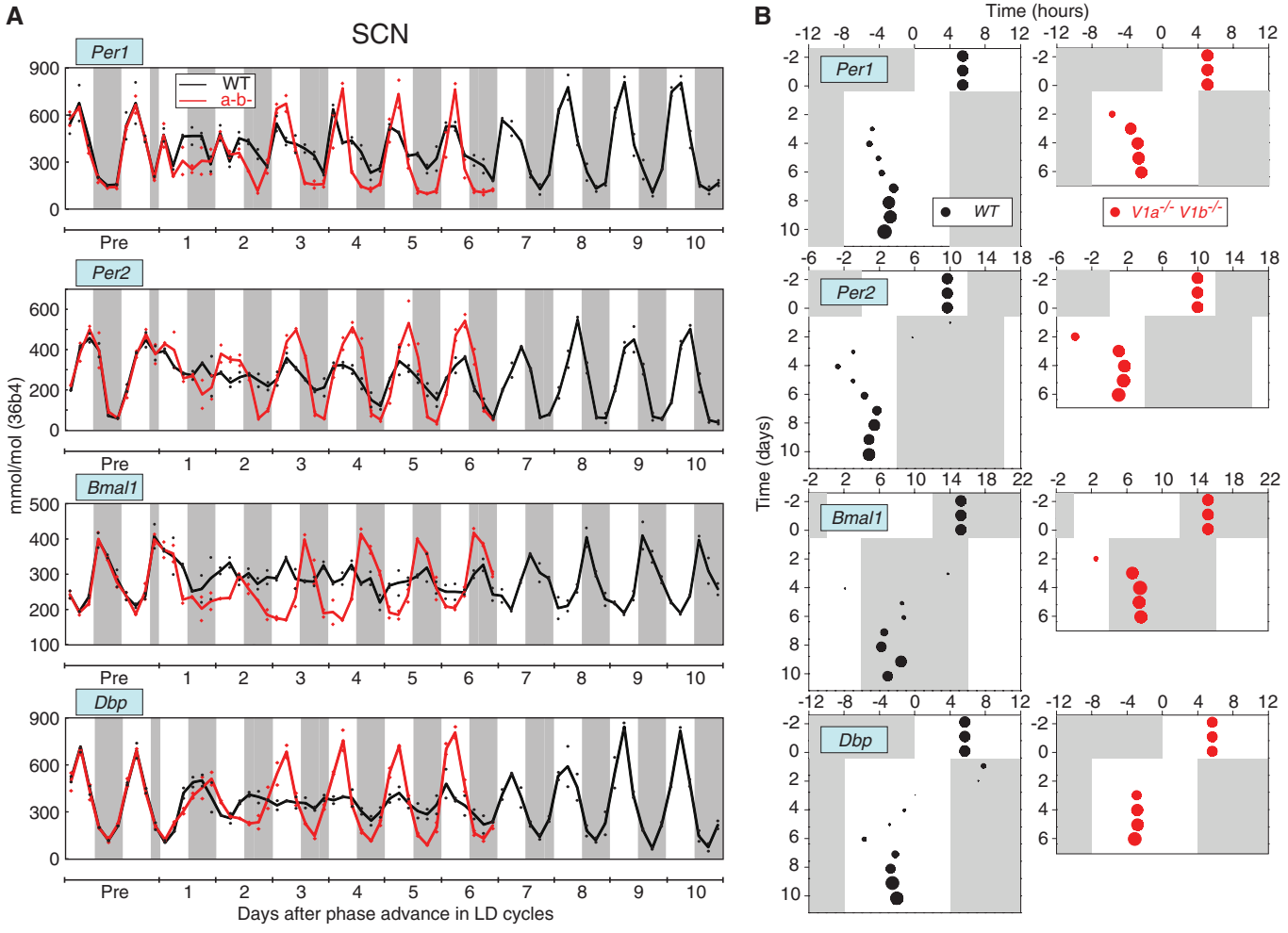

Fig. 2. $V1a^{-/-}V1b^{-/-}$ mice subjected to an experimental jet-lag paradigm show fast reentrainment of SCN clock gene rhythms. (**A**) Measurement by qRT-PCR of clock gene expression profiles (*Per1*, *Per2*, *Bmal1*, and *Dbp*) in the laser microdissected SCN (fig. S8A), obtained every 4 hours continuously throughout the jet-lag schedule (fig. S8B). LD cycles were advanced by 8 hours on day 1. Graph indicates an average of two mice independently collected and measured. Note that all transcripts examined in WT SCN lost rhythmicity right after jet lag. (**B**) Peak time- and amplitude-based kinetic analyses of reentrainment in clock gene expression rhythms. Peak time and amplitude are shown schematically as dots, position and diameter representing peak time and daily amplitude, respectively. Dots were omitted when daily peak time was ambiguous. Dots before an 8-hour phase advance are triple-plotted for better visualization. Black and red colors indicate WT and $V1a^{-/-}V1b^{-/-}$, respectively.

alterations in AVP-mediated interneuronal communication in the SCN. To investigate the effect of AVP-mediated communication on cellular rhythms, we performed real-time bioluminescence imaging of SCN slices from WT and *V1a*$^{-/-}$*V1b*$^{-/-}$ mice carrying *Per1*-promoter–luciferase (*Per1-luc*), which allows simultaneous measurement of hundreds of cellular rhythms (*8*). Both WT and *V1a*$^{-/-}$*V1b*$^{-/-}$ SCN neurons showed robust rhythms in a spatiotemporally organized manner, starting from the dorsomedial portion and spreading to the ventrolateral side (Fig. 4 and movies S1 and S2). This phase order was perturbed by administration of cycloheximide (CHX), which resets the phase of all neurons (*8*). After CHX withdrawal, the original phase order among WT neurons recovered, whereas that among *V1a*$^{-/-}$*V1b*$^{-/-}$ neurons was severely permuted (Fig. 4, fig. S16, and Movie S3). These results indicate that *V1a*$^{-/-}$*V1b*$^{-/-}$ SCN is more amenable to perturbation than WT SCN. Conceivably, it is this vulnerability in interneuronal coupling that enables the mutant SCN to reentrain to altered lighting schedules more rapidly.

To evaluate the effect of AVP-mediated cellular interaction in the SCN under jet-lag conditions, we built a mathematical model consisting of three oscillators in the SCN and one in the

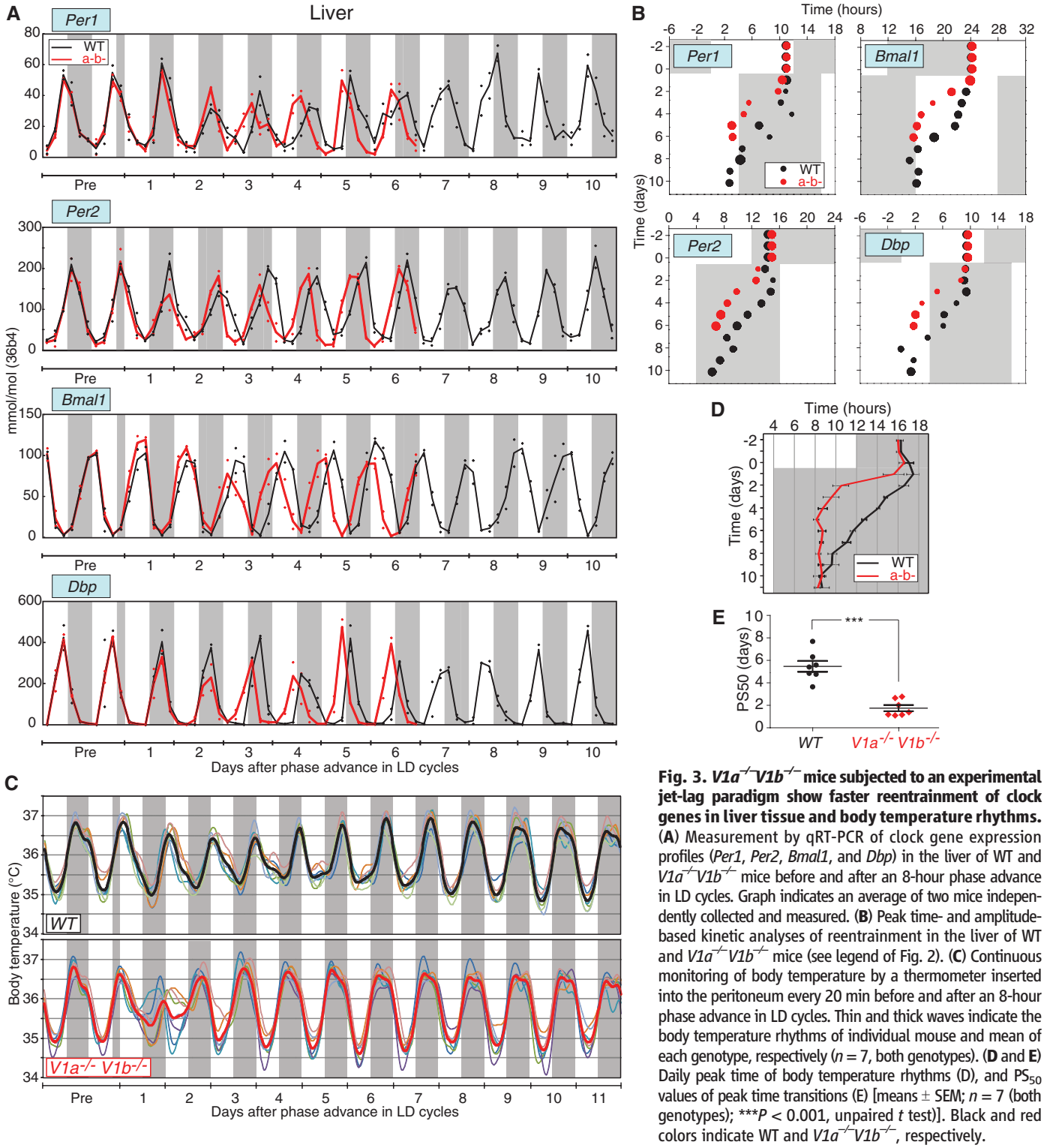

Fig. 3. *V1a*$^{-/-}$*V1b*$^{-/-}$ mice subjected to an experimental jet-lag paradigm show faster reentrainment of clock genes in liver tissue and body temperature rhythms. (**A**) Measurement by qRT-PCR of clock gene expression profiles (*Per1*, *Per2*, *Bmal1*, and *Dbp*) in the liver of WT and *V1a*$^{-/-}$*V1b*$^{-/-}$ mice before and after an 8-hour phase advance in LD cycles. Graph indicates an average of two mice independently collected and measured. (**B**) Peak time- and amplitude-based kinetic analyses of reentrainment in the liver of WT and *V1a*$^{-/-}$*V1b*$^{-/-}$ mice (see legend of Fig. 2). (**C**) Continuous monitoring of body temperature by a thermometer inserted into the peritoneum every 20 min before and after an 8-hour phase advance in LD cycles. Thin and thick waves indicate the body temperature rhythms of individual mouse and mean of each genotype, respectively ($n = 7$, both genotypes). (**D** and **E**) Daily peak time of body temperature rhythms (D), and PS_{50} values of peak time transitions (E) [means ± SEM; $n = 7$ (both genotypes); ***$P < 0.001$, unpaired t test)]. Black and red colors indicate WT and *V1a*$^{-/-}$*V1b*$^{-/-}$, respectively.

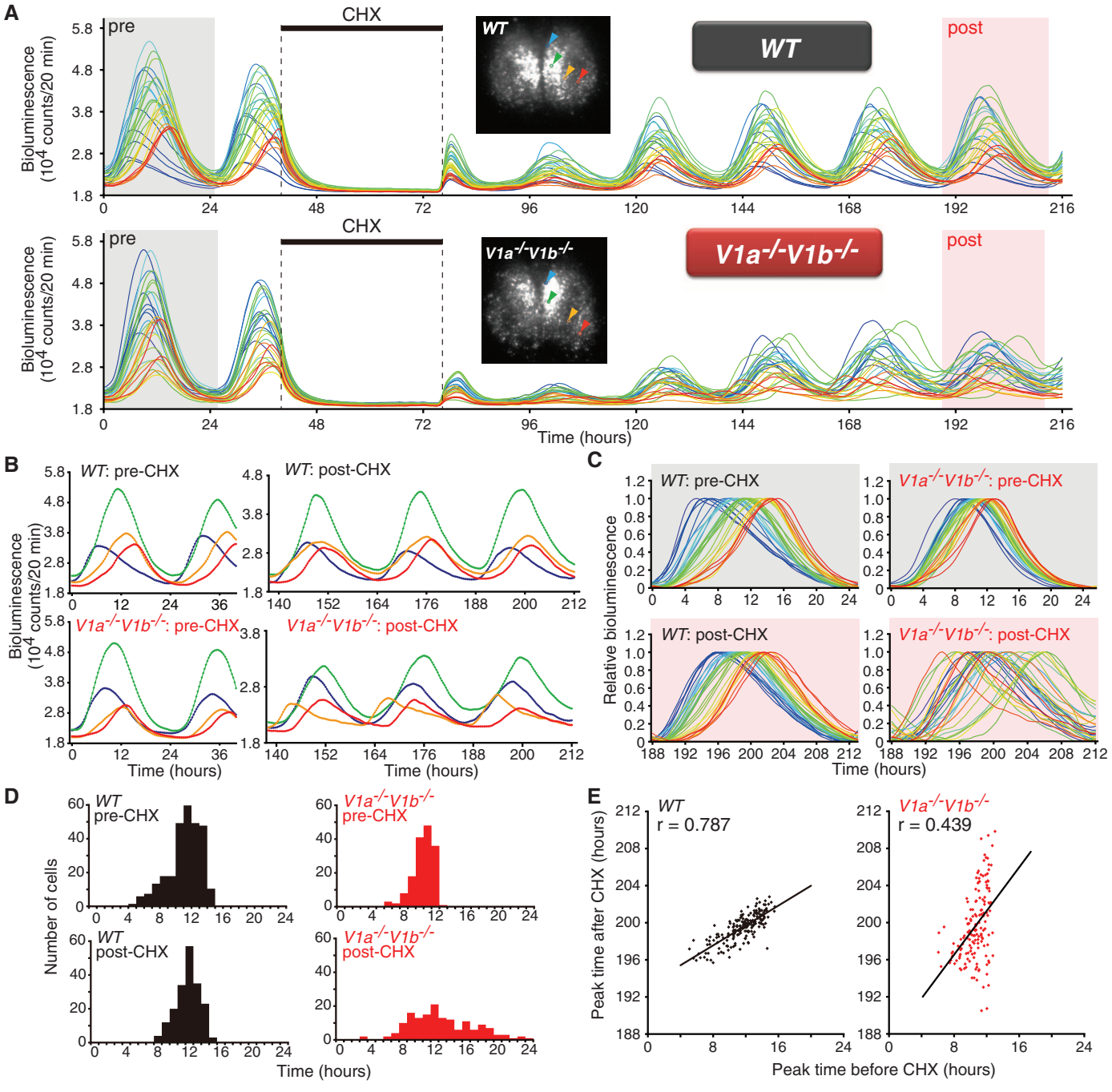

Fig. 4. Perturbation experiments with CHX reveal a weak spatiotemporal phase order organization in the SCN of *V1a*$^{-/-}$*V1b*$^{-/-}$ mice. (**A**) Representative cellular rhythms randomly chosen over the SCN slice (29 cells, both genotypes). Cellular oscillations showed a stable phase order in each cycle, but all cell clocks were reset with CHX application, and the first peaks of cells appeared simultaneously at 3 hours after CHX washout in both WT and *V1a*$^{-/-}$*V1b*$^{-/-}$ SCN. The phase order among the individual cells gradually recovered cycle by cycle in WT, whereas phases of cellular oscillations were severely permuted in *V1a*$^{-/-}$*V1b*$^{-/-}$ SCN. (**B**) Recording of bioluminescence of four representative cells pre- (0 to 40 hours) and post- (138 to 212 hours) CHX treatment [see inset photos in (A) for localization of cells; scale bar, 100 μm]. Note the phase order of four cells (blue-green-orange-red) was maintained before and after CHX treatment in WT SCN, but it was not in *V1a*$^{-/-}$*V1b*$^{-/-}$ SCN. (**C**) Normalized bioluminescence of individual cells during pre- [0 to 24 hours in (A), gray background] and post- [188 to 212 hours in (A), pink background] CHX treatment. Peak and trough values were adjusted to 1 and 0, respectively. (**D**) The range of peak times of randomly chosen cells [n = 180 (WT) and 155 (*V1a*$^{-/-}$*V1b*$^{-/-}$)] before and after CHX treatment. The x axis represents circadian hours (1 hour = peak interval/24 hours) from the trough time of the total SCN bioluminescence. (**E**) Correlation of the peak times of the individual cells [n = 180 (WT) and 155 (*V1a*$^{-/-}$*V1b*$^{-/-}$)] before CHX application (0 to 24 hours) with those after CHX washout (188 to 212 hours). Strong correlation in peak times before and after CHX treatment was observed in WT SCN, but not in *V1a*$^{-/-}$*V1b*$^{-/-}$ SCN. The results shown are representative of four independent experiments that yielded similar results.

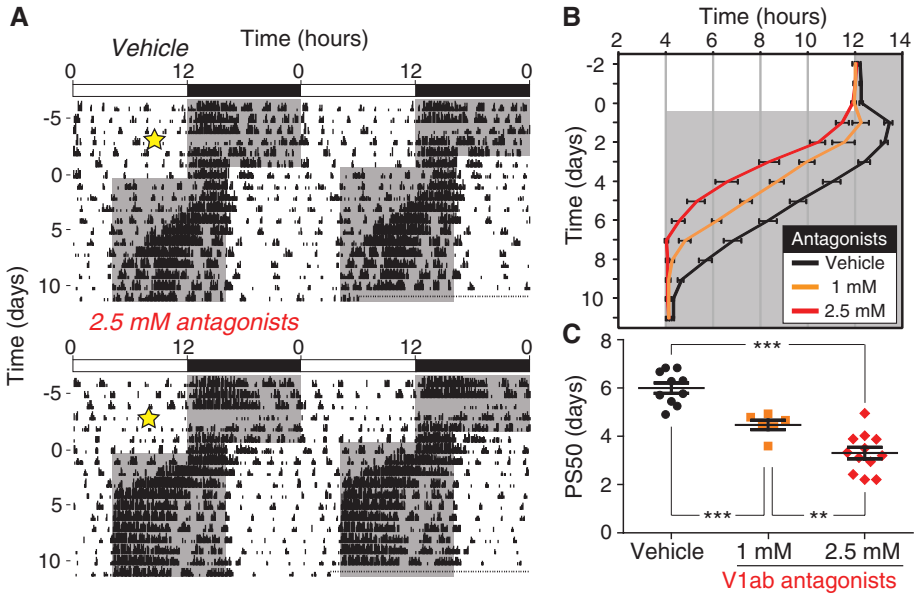

Fig. 5. Direct infusion of V1a and V1b antagonists into the SCN enhances the speed of reentrainment of WT mice subjected to an experimental jet-lag paradigm. (**A** to **C**) A mixture of OPC-21268 (V1a antagonist) and SSR 149415 (V1b antagonist) was applied over the SCN by osmotic minipump, and LD cycles were advanced by 8 hours on day 1. Two concentrations of each antagonist (1 mM or 2.5 mM) were applied. (A) Representative double-plotted actograms of vehicle- (top) or 2.5 mM antagonist-treated mice (bottom). Time of surgery is indicated by a yellow star. (B) Activity onset [means ± SEM; n = 10, 6, and 12 in vehicle, 1 mM, and 2.5 mM groups, respectively). (C) PS_{50} values of onset time transitions (means ± SEM). One-way analysis of variance (ANOVA), $F_{2,25} = 39.09$; $P < 0.0001$. Tukey-Kramer post hoc test was performed for comparison among the groups. $^{**}P < 0.01$, $^{***}P < 0.001$.

periphery. This model is based on a phase oscillator (*26*, *27*) and is useful for understanding the dynamics of coupled multiple oscillators (see fig. S17 and supplementary text for details). This model showed that the WT SCN output lost rhythmicity for several days, whereas that of $V1a^{-/-}V1b^{-/-}$ recovered quickly after a phase advance in LD cycles (fig. S17, C and D). Faster reentrainment of peripheral output in $V1a^{-/-}V1b^{-/-}$ compared with WT was also recreated in our model (fig. S17, E and F).

Pharmacological Inhibition of V1a/V1b Signaling

Our mathematical model predicted that the weaker the AVP-mediated intercellular communication becomes, the shorter the reentrainment period (fig. S18). To test this experimentally, we transiently blocked V1a and V1b signaling in the SCN of adult WT mice in vivo during jet lag. We applied a mixture of OPC-21268 (V1a antagonist) and SSR 149415 (V1b antagonist) just over the SCN through an osmotic minipump (*28*). Mice receiving this treatment reentrained significantly faster to new LD cycles in a dose-dependent manner (Fig. 5). To examine the effect of these antagonists on the assembly of cellular rhythms among SCN neurons, we treated WT SCN slices with a mixture of antagonists after CHX application and found that the original phase order among WT SCN neurons was severely permuted as observed in $V1a^{-/-}V1b^{-/-}$ SCN (fig. S19). These results support the crucial role of V1a and V1b signaling in the SCN in determining the speed of reentrainment after a phase advance in LD cycles and exclude the possibility that rapid reentrainment in $V1a^{-/-}V1b^{-/-}$ mice is simply caused by a developmental failure in mutant mice.

Conclusions

In summary, we have shown that mice lacking the vasopressin V1a and V1b receptors are resistant to jet lag, as measured by locomotor activity, clock gene expressions, and body temperature. The mutant mice rapidly phase-shift to a new environmental LD cycle. Like AVP and its receptors, vasoactive intestinal polypeptide and its receptor VPAC2 are also expressed in the SCN and have been linked to the circadian clock. However, deficiency of VPAC2 in mice has severe consequences on behavior and neural activity rhythms, as well as clock gene oscillations (*10*, *29*). In contrast, we showed that the absence of V1a and V1b receptors does not elicit overt anomalies in behavioral and clock gene expression rhythms under regular LD and constant DD conditions. Previous work suggested that genetic manipulation of AVP or its receptor have only minor effects on circadian behavior (*19*, *30*). Here, however, we demonstrated that rhythms of behavior, clock gene oscillation, and body temperature in $V1a^{-/-}V1b^{-/-}$ mice reentrain immediately after a phase advance in LD cycles. We hypothesize that this occurs because AVP-mediated interneuronal communication, which confers on the SCN an intrinsic resistance to external perturbations like jet lag, is missing in $V1a^{-/-}V1b^{-/-}$ mice.

Epidemiological studies have shown that chronic jet lag and rotating shift work can increase an individual's risk of developing hypertension, obesity, and other metabolic disorders. Our results identify vasopressin signaling as a possible therapeutic target for the management of circadian rhythm misalignment.

References and Notes

1. C. A. Comperatore, G. P. Krueger, *Occup. Med.* **5**, 323–341 (1990).
2. R. L. Sack, *Travel Med. Infect. Dis.* **7**, 102–110 (2009).
3. O. M. Buxton *et al.*, *Sci. Transl. Med.* **4**, 129ra43 (2012).
4. F. A. Scheer, M. F. Hilton, C. S. Mantzoros, S. A. Shea, *Proc. Natl. Acad. Sci. U.S.A.* **106**, 4453–4458 (2009).
5. S. Kiessling, G. Eichele, H. Oster, *J. Clin. Invest.* **120**, 2600–2609 (2010).
6. S. Yamazaki *et al.*, *Science* **288**, 682–685 (2000).
7. A. B. Reddy, M. D. Field, E. S. Maywood, M. H. Hastings, *J. Neurosci.* **22**, 7326–7330 (2002).
8. S. Yamaguchi *et al.*, *Science* **302**, 1408–1412 (2003).
9. J. A. Mohawk, J. S. Takahashi, *Trends Neurosci.* **34**, 349–358 (2011).
10. S. J. Aton, C. S. Colwell, A. J. Harmar, J. Waschek, E. D. Herzog, *Nat. Neurosci.* **8**, 476–483 (2005).
11. M. P. Butler, R. Silver, *J. Biol. Rhythms* **24**, 340–352 (2009).
12. E. S. Maywood, J. E. Chesham, J. A. O'Brien, M. H. Hastings, *Proc. Natl. Acad. Sci. U.S.A.* **108**, 14306–14311 (2011).
13. R. Cao, G. Q. Butcher, K. Karelina, J. S. Arthur, K. Obrietan, *Eur. J. Neurosci.* **37**, 130–140 (2013).
14. H. Okamura, *Cold Spring Harb. Symp. Quant. Biol.* **72**, 551–556 (2007).
15. A. N. van den Pol, K. L. Tsujimoto, *Neuroscience* **15**, 1049–1086 (1985).
16. W. J. Schwartz, S. M. Reppert, *J. Neurosci.* **5**, 2771–2778 (1985).
17. D. F. Swaab, C. W. Pool, F. Nijveldt, *J. Neural Transm.* **36**, 195–215 (1975).
18. W. S. Young 3rd, K. Kovács, S. J. Lolait, *Endocrinology* **133**, 585–590 (1993).
19. J. D. Li, K. J. Burton, C. Zhang, S. B. Hu, Q. Y. Zhou, *Am. J. Physiol. Regul. Integr. Comp. Physiol.* **296**, R824–R830 (2009).
20. T. A. Koshimizu *et al.*, *Proc. Natl. Acad. Sci. U.S.A.* **103**, 7807–7812 (2006).
21. A. Tanoue *et al.*, *J. Clin. Invest.* **113**, 302–309 (2004).
22. Materials and methods are available as supplementary material on *Science* Online.
23. X. Jin *et al.*, *Cell* **96**, 57–68 (1999).
24. M. Castel, N. Feinstein, S. Cohen, N. Harari, *J. Comp. Neurol.* **298**, 172–187 (1990).
25. T. Kalamatianos, I. Kalló, C. W. Coen, *J. Neuroendocrinol.* **16**, 493–501 (2004).
26. A. T. Winfree, *J. Theor. Biol.* **16**, 15–42 (1967).
27. Y. Kuramoto, *Chemical Oscillations, Waves, and Turbulence* (Dover Publications, New York, 2003).
28. M. Doi *et al.*, *Nat. Commun.* **2**, 327 (2011).
29. A. J. Harmar *et al.*, *Cell* **109**, 497–508 (2002).
30. T. A. Groblewski, A. A. Nunez, R. M. Gold, *Brain Res. Bull.* **6**, 125–130 (1981).

Acknowledgments: This work was supported in part by Grant-in-Aid for Specially Promoted Research (to H.O.) and Scientific Research on Innovative Areas "Brain Environment" (to H.O.) from the Ministry of Education, Science, Sports and Culture of Japan, and by grants from Takeda Science Foundation (to H.O.), SRF (to H.O.), and Kanae Science Foundation (to Y.Y.). H.O. and Kyoto University have applied for a patent (PCT/JP2013/064376) related to the use of V1a and V1b antagonists as circadian rhythm modulators.

Supplementary Materials

www.sciencemag.org/content/342/6154/85/suppl/DC1
Materials and Methods
Supplementary Text
Figs. S1 to S19
References (*31*–*44*)
Movies S1 to S3

1 April 2013; accepted 22 August 2013
10.1126/science.1238599